https://doi.org/10.22226/2410-3535-2022-3-191-196

Check for updates

Thermal properties of nanocrystalline copper sulfides $K_xCu_{1.85}S$ ($0 < x < 0.05$)

K. A. Kuterbekov[1], M. Kh. Balapanov[2], M. M. Kubenova[1], R. Sh. Palymbetov[1], R. Kh. Ishembetov[2], S. M. Sakhabayeva[1], A. M. Kabyshev[†,1], B. M. Akhmetgaliev[2], K. Zh. Bekmyrza[1], Ye. T. Abseitov[1], Sh. G. Giniyatova[1]

[†]assetenu@gmail.com

[1]L. N. Gumilyov Eurasian National University, Nur-Sultan, 010008, Kazakhstan
[2]Bashkir State University, Ufa, 450076, Russia

This paper presents the comparative data on thermal properties of five compounds of nanocrystalline copper sulfides $K_xCu_{1.85}S$ ($0 < x < 0.05$) at the temperature range from 300 to 700 K. X-ray phase analysis shows that $Cu_{31}S_{16}$ (or $Cu_{1.9375}S$) monoclinic djurleite phase are found as prevailing in all $K_xCu_{1.85}S$ samples ($0.01 < x < 0.05$). Also in all samples there are oxygen oxide Cu_2O and orthorhombic anilite Cu_7S_4 ($Cu_{1.75}S$). Variable components of the alloys are monoclinic and hexagonal chalcocite, triclinic roxbyite. The sizes of crystallites in the alloys estimated from half-width of X-ray lines are in the range from 11 to 265 nm at room temperature. Differential scanning calorimetry revealed considerable endothermic thermal effect in the temperature range from 370 to 375 K for all compounds, obviously caused by the superionic phase transition from monoclinic djurleite to hexagonal chalcocite. The thermal conductivity of alloys decreases to $0.16 \div 0.25$ W K^{-1}m^{-1} in the temperature range of 450 – 600 K due to an increase in the amount of potassium (for $x = 0.04$, 0.05). This favors the achievement of high thermoelectric figure of merit of the material. The obtained results are important for semiconductor materials used in the field of thermoelectric devices.

Keywords: nanocrystalline copper sulfides, thermal conductivity, X-ray phase analysis, differential scanning calorimeter, differential thermal analysis, heat capacity, figure of merit *ZT*.

1. Introduction

Increasing global demand for sustainable energy makes a huge contribution to the development of the thermoelectric industry. Over the past decade, these achievements of researchers aroused a growing interest in this area to obtain highly efficient thermoelectric materials (from complexity in a single cell to nanostructured bulk and thin-film materials) that were made through a wide range of new approaches [1 – 3].

The efficiency of these devices is determined by a dimensionless quantity called figure-of-merit, $ZT = \alpha^2\sigma T/\chi$, where Z is the thermoelectric figure of merit, T is the absolute temperature, α is the Seebeck coefficient, σ is the electrical conductivity, which determine the maximum produced thermoelectric power $P = \alpha^2\sigma$, and χ is the total thermal conductivity, which characterizes energy losses in the converter: $Z = P/\chi = \alpha^2\sigma/\chi$ [4 – 6].

Thermoelectric materials can have the best value of the dimensionless thermoelectric characteristic *ZT* only with an optimal set of three values — the Seebeck coefficient, electronic conductivity and thermal conductivity, related to each other through the Fermi level, the effective mass of carriers and other parameters of the semiconductor. Significant efforts are needed to improve the *ZT* of known materials, and even more so to discover new thermoelectric materials. One traditional way to improve *ZT* is to reduce the thermal conductivity χ via alloying, which does not significantly reduces the electrical properties [7].

Recently, there have been interesting and thorough review articles on various families of materials such as sulfides [8], oxides, chalcogenides [9 – 10], graphene-based materials, silicon, polymers, or composites [11], as well as the latest developments in thermoelectric materials for various structures, as, for example, nanostructured materials, layered materials, 2D materials [12]. Of great interest are publications on wearable thermoelectric power generators in combination with a flexible supercapacitor [13 – 14]. Superionic copper sulfides and their alloys are promising thermoelectric materials [15]. The low thermal conductivity of these systems is provided by the suppression of phonon transfer in a "liquid-like" cationic substrate that does not suppress electron transfer. Thermal conductivity in thermoelectric materials is provided by electrons and holes that transfer heat and/or by phonons propagating along the crystal lattice [16].

There are few works on the physical properties of potassium-containing copper sulfides in the literature. The work by Lee [17] reports on $KCu_{7-x}S_4$ nanowires demonstrating enhanced thermoelectric properties in comparison with binary Cu_7S_4 nanocrystals. Low thermal conductivity (less

than 0.5 $W m^{-1}K^{-1}$ in the range 325 – 575 K) was observed when nanowires were pressed into a bulk material. The peak values of thermoelectric figure of merit are obtained for $KCu_{7-x}S_4$: $ZT = 0.12$ at 350 K, $ZT = 0.19$ at 575 K.

The work [18] presents the results of studies on the $K_{0.2}Cu_{1.8}S$ alloy in the temperature range from 300 to 670 K. Above 570 K in $K_{0.2}Cu_{1.8}S$, a strong increase in the thermo-emf coefficient was observed (up to 4 mV/K) and a decrease in thermal conductivity to 0.4 $W K^{-1}m^{-1}$, leading to a extremely high peak value $ZT = 3.5$ at 650 K.

The paper [19] presents the results of experimental studies of electronic conductivity and Seebeck coefficient, thermal conductivity in $K_xCu_{2-x}S$ ($x = 0.1$, 0.2, 0.25) alloy samples in the temperature range from 300 to 690 K. In the temperature range above room temperature for all samples, the authors found a semiconductor nature of conductivity, which then changes to metallic one (above 372, 363 and 540 K for alloys $K_{0.1}Cu_{1.9}S$, $K_{0.2}Cu_{1.8}S$, $K_{0.25}Cu_{1.75}S$, respectively). The activation energy of the conductivity was found to be equal to 0.16, 0.22 and 0.39 eV for $K_{0.1}Cu_{1.9}S$, $K_{0.2}Cu_{1.8}S$ and $K_{0.25}Cu_{1.75}S$ respectively. In the range from 400 to 540 K, the activation energy of the $K_{0.25}Cu_{1.75}S$ alloy decreased to 0.16 eV. The thermal conductivity coefficients of $Li_xCu_{2-x}S$ alloys in the studied temperature range have low values, from 1.1 to 0.2 $W K^{-1}m^{-1}$. The abnormally high peak of the Seebeck coefficient found in the studied alloys at 630 – 650 K might be due to the superionic phase transition from the hexagonal phase to the cubic one of those alloy fractions that were in rhombohedral ($Cu_{17}S_9$) and tetragonal (Cu_2S) modifications at room temperature, and then transformed into hexagonal modifications $Cu_{17}S_9$ and Cu_2S, respectively, at 354 and 363 K.

Roseboom [20] studied the phase stability of the Cu-S system over a wide temperature range. According to him, copper, chalcocite (Cu_2S), djurleite (about $Cu_{1.96}S$), and digenite solid solution ($Cu_{1.79}S$ to $Cu_{1.765}S$) are stable phases at 298 K. Above 298 K, the equilibrium copper content of digenite ("high digenite" above 349 – 356 K) increases with temperature until it reaches Cu_2S composition at about 708 K, the inversion temperature of hexagonal chalcocite to high digenite. Hexagonal chalcocite is stable with high digenite down to 366 ±1.5 K and with copper down to 376.5 ±1.5 K. Chalcocite (Cu_2S) is stable below 376.5 K. Both natural and synthetic djurleite break down at 366 ±1.5 K to hexagonal chalcocite ($Cu_{1.988}S$) plus high digenite ($Cu_{1.84}S$); this process occurs reversibly.

In this paper, we investigate thermoelectric phenomena in an environmentally friendly superionic copper sulfide material doped with potassium to obtain an optimal electron concentration in order to achieve maximum thermoelectric power. Data on thermal properties of potassium-doped copper sulfide $K_xCu_{1.85}S$ ($0 < x < 0.05$), and its phase composition are presented.

2. Materials and methods

There are three main methods that are commonly used to densify nanostructured materials: cold pressing followed by sintering, hot uniaxial pressing (hot pressing), and spark plasma sintering (SPS). A relatively new method that can be used to sinter "softer" materials is known as incineration densification. Here, cold pressing used to densify the materials. In cold pressing followed by sintering, materials are loaded into a mold (usually stainless steel) and hydrostatic pressures of about 5 tons are applied, typically using a Carver press. The pellets are then extracted and heated to about 70% of the theoretical melting point to sinter the nanopowder. If everything is done correctly, it is possible to obtain samples with a density of up to 90 percent of the theoretical one [21].

In this work, semiconducting alloys $K_xCu_{1.85}S$ ($x = 0.01$, 0.02, 0.03, 0.04, 0.05) were synthesized in a melt of a mixture of NaOH and KOH hydroxides at a temperature of about 165°C. As a result of the synthesis, a potassium-doped copper sulfide nanopowder is obtained. The materials are compacted by cold pressing followed by annealing in argon at 450°C. The methods of X-ray phase analysis, differential scanning calorimetry and electron microscopy are used to characterize the structure and properties of materials.

The heat capacity was measured on a DSC404 NETZSCH DSC calorimeter at a heating rate of 10 K/min in a dry argon atmosphere. The thermal diffusivity and thermal conductivity of solid samples were measured using the LFA 467 HT HyperFlash instrument (NETZSCH, Germany).

3. Results and Discussion

3.1. X-ray phase analysis

Figure 1 illustrates the X-ray phase lines of the nanocrystalline copper sulfide alloys $K_xCu_{1.85}S$ ($0 < x < 0.05$).

The XRD patterns show that $Cu_{31}S_{16}$ (or $Cu_{1.9375}S$) monoclinic djurleite phase are found as prevailing in all $K_xCu_{1.85}S$ samples ($0.01 < x < 0.05$). Also in all samples there are oxygen oxide Cu_2O and orthorhombic anilite Cu_7S_4 ($Cu_{1.75}S$). Variable components of the alloys are monoclinic and hexagonal chalcocite, triclinic roxbyite. The sizes of crystallites in the alloy are in the range from 11 to 265 nm. These data are in good agreement with our previous data analyses that the samples of $K_xCu_{1.97-x}S$ at room temperature were also a mixture of different phases of copper sulfide. In [22], the crystallite sizes calculated from the half-width of the X-ray lines were in the ranges 10 to 64 nm for $K_{0.01}Cu_{1.96}S$ and 7 to 47 nm for $K_{0.05}Cu_{1.94}S$. The sizes of crystallites in $K_xCu_{1.85}S$ ($x = 0.01$, 0.02, 0.03, 0.04, 0.05) alloys calculated from the half-width of X-ray lines are shown in Table 1.

3.2. Differential Scanning Calorimetry

The DSC curves of the alloys are presented in Fig. 2. They show a considerable endothermic thermal effect in the temperature range from 370 to 375 K, which is seen for all compounds. The main phase of our alloys — monoclinic djurleite break down at 366 ±1.5 K to hexagonal chalcocite ($Cu_{1.988}S$) plus high digenite ($Cu_{1.84}S$) [20], and according to Chakrabarti [23] the phase transition from monoclinic djurleite to superionic hexagonal chalcocite occurs in coarse-grained materials at about 370 K. In nanosized copper sulfide (with a size of 4 – 5 nm), the phase transition temperature can decrease by up to 60 – 70 degrees [24, 25]. The orthorhombic anilite $Cu_{1.75}S$ transforms to low-digenite

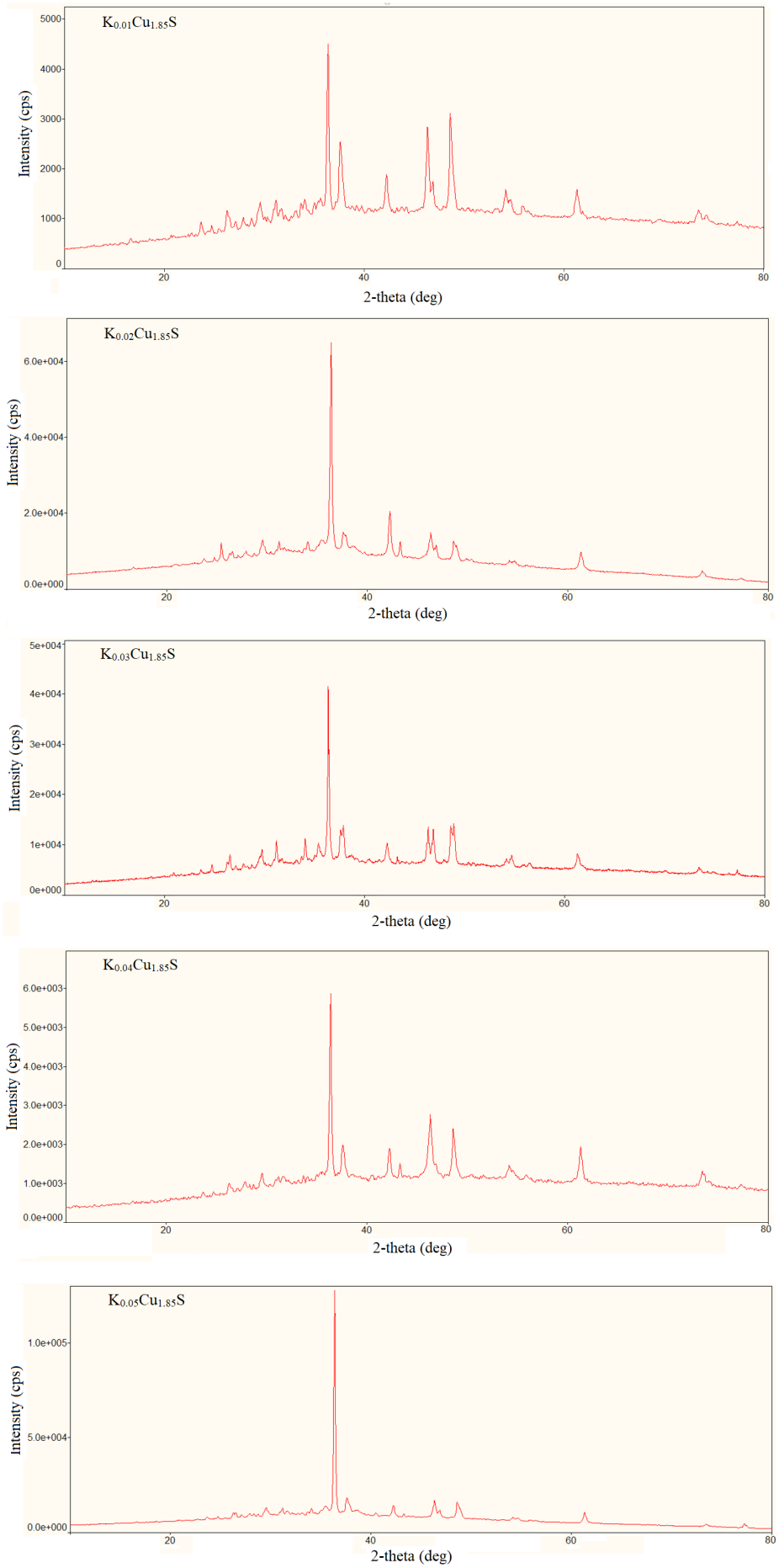

Fig. 1. X-ray spectra of samples $K_xCu_{1.85}S$ (x = 0.01, 0.02, 0.03, 0.04, 0.05).

Table 1. Sizes of crystallites in $K_xCu_{1.85}S$ ($x = 0.01, 0.02, 0.03, 0.04, 0.05$) alloys calculated from the X-ray line half-width.

Phase	Phase name	Crystal System	Phase content in sample	Crystallite size range, nm
$K_{0.01}Cu_{1.85}S$				
$Cu_{31}S_{16}$	Djurleite	Monoclinic	70%	19–150
Cu_2O	Copper oxide (I)	Cubic	15%	20–50
Cu_7S_4	Anilite	Orthorhombic	9%	29–73
Cu_2S	Chalcocite	Hexagonal	6%	28–39
$K_{0.02}Cu_{1.85}S$				
$Cu_{31}S_{16}$	Djurleite	Monoclinic	63%	11–135
$Cu_{29}S_{16}$	Roxbyite	Triclinic	8%	39–73
Cu_2S	Chalcocite	Monoclinic	5%	39–49
Cu_7S_4	Anilite	Orthorhombic	7%	26–84
$K_{0.03}Cu_{1.85}S$				
$Cu_{31}S_{16}$	Djurleite	Monoclinic	68%	13–136
Cu_2O	Copper oxide (I)	Cubic	16%	20–104
$Cu_{29}S_{16}$	Roxbyite	Triclinic	7%	40–116
Cu_7S_4	Anilite	Orthorhombic	9%	38–120
$K_{0.04}Cu_{1.85}S$				
$Cu_{31}S_{16}$	Djurleite	Monoclinic	74%	12–265
Cu_2O	Copper oxide (I)	Cubic	15%	24–84
Cu_2S	Chalcocite	Monoclinic	7%	33–42
Cu_7S_4	Anilite	Orthorhombic	4%	33–117
$K_{0.05}Cu_{1.85}S$				
$Cu_{31}S_{16}$	Djurleite	Monoclinic	77%	14–120
Cu_2O	Copper oxide (I)	Cubic	19%	27–102
Cu_7S_4	Anilite	Orthorhombic	4%	35–56

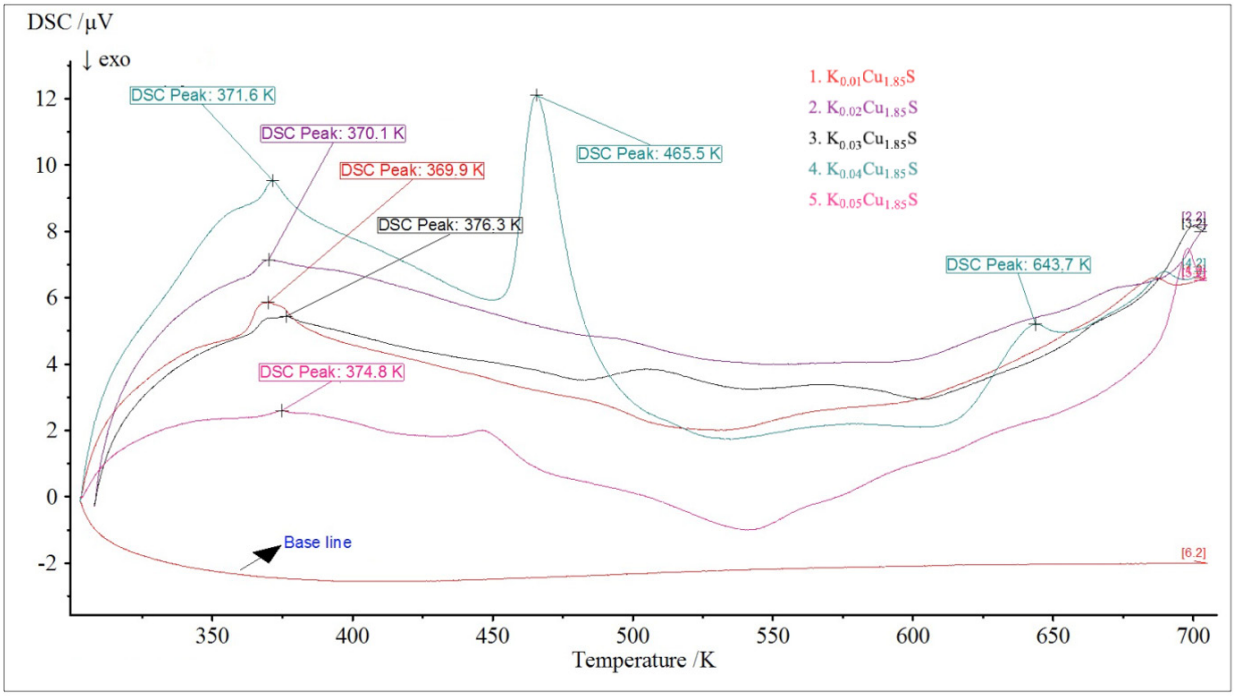

Fig. 2. (Color online) The DSC curves of the $K_xCu_{1.85}S$ ($x = 0.01, 0.02, 0.03, 0.04, 0.05$) samples in temperature range of 300–700 K.

at 348 ± 3 K [23], but this effect is not visible on Fig. 2 as the content of anilite in the alloys is small.

The DSC curve for $K_{0.04}Cu_{1.85}S$ compound shows a sharp peak of the endothermic thermal effect at a temperature of about 465 K, the origin of which is unknown. In [17], endothermic DSC peaks at 448 and 451 K were obtained for $K_{0.25}Cu_{1.70}S$ and $Cu_{1.75}S$ nanocrystals. The reason for these effects is unclear and needs to be studied.

The measurements showed a decrease in the minimum value of thermal conductivity with an increase in the potassium content in the composition, which can be associated with an increase in phonon scattering with an increase in the concentration of scattering impurity ions. DTA [26] and DSC revealed a superionic phase transition from an ordered low-symmetry djurleite phase to a disordered superionic hexagonal copper sulfide phase at a temperature

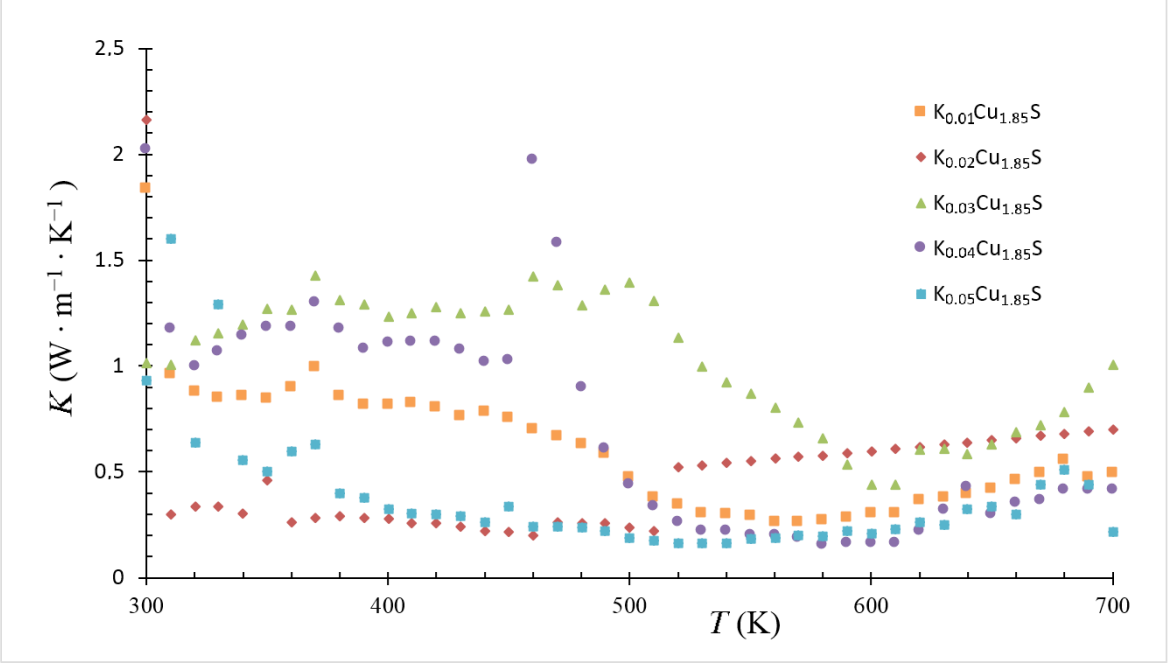

Fig. 3. (Color online) Temperature dependences of the thermal conductivity coefficient of $K_xCu_{1.85}S$ (x = 0.01, 0.02, 0.03, 0.04, 0.05).

of about 370 – 376 K. The "molten" cationic sublattice creates phonon glass conditions and suppresses phonon propagation without interfering with electron transfer.

3.3. Thermal conductivity

Figure 3 illustrates the thermal conductivity graph of the $K_xCu_{1.85}S$ (x = 0.01, 0.02, 0.03, 0.04, 0.05) samples in temperature range of 300 – 700 K.

In [27], the total thermal conductivity value of $Yb_{14}MnSb_{11}$ showed a downward trend, reaching a low point of 0.7 W m^{-1}K^{-1} at temperature range of 300 – 1275 K. In contrast, in our study, the thermal conductivity value in alloys $K_xCu_{1.85}S$ (x = 0.01, 0.02, 0.03, 0.04, 0.05) indicated low point values from 0.2 W m^{-1}K^{-1} in $K_{0.01}Cu_{1.85}S$ to 0.16 W m^{-1}K^{-1} in $K_{0.04}Cu_{1.85}S$ at 600 K (it is comparatively equal to the glass limit), and this is expected to have a significant impact on the high level of the figure of merit of material. Reduction in the electronic contribution leads to a very low level of the thermal conductivity of the material, such low values can be obtained through the limiting of the free movement of phonons and reducing the share of atomic oscillatory modes that effectively conduct heat [28].

Additional factors for reducing the total thermal conductivity in the studied alloys are mixed potassium ions, which lead to an increase in the scattering of phonons and electrons, as well as nanosizes of grains, which increases the number of structural defects at the phase boundaries [29].

4. Conclusion

At room temperature, the semiconductor alloys $K_xCu_{1.85}S$ (x = 0.01, 0.02, 0.03, 0.04, 0.05) are composed of a mixture of copper sulfide phases. Four phases were revealed in the samples: djurleite $Cu_{31}S_{16}$, chalcocite Cu_2S, roxbyite $Cu_{29}S_{16}$, anilite Cu_7S_4, with monoclinic djurleite being the predominant phase of the alloys.

According to estimates from the X-ray phase lines of the nanocrystalline copper sulfide alloys, the sizes of crystallites in the alloy range from 11 to 256 nm.

The results of X-ray phase analysis are confirmed by differential scanning thermometry, which recorded thermal effects correspond to phase transition from monoclinic djurleite to superionic hexagonal chalcocite around 370 K.

As a result, we obtained minimum values of thermal conductivity of about 0.16 W m^{-1}K^{-1} in $K_{0.04}Cu_{1.85}S$ at 600 K, which are comparable to the glass limit values for the lattice component of thermal conductivity. It resulted in a very high peak value of dimensionless thermoelectric efficiency ZT = 9.67 for $K_{0.04}Cu_{1.85}S$ composition at 620 K [30].

We compared and analyzed the obtained data with previous materials and focused on the estimation of the thermal conductivity of the nanocrystalline copper sulfides, and it is expected that the obtained data will enhance the performance of thermoelectric materials.

Acknowledgements. This research was funded by the Science Committee of the Ministry of Education and Science of the Republic of Kazakhstan (No. AP08856636).

References

1. J. G. Snyder, E. S. Toberer. Nature materials. 7, 105 (2008). Crossref
2. O. Caballero-Calero, J. R. Ares, M. Martin-González. Adv. Sustainable Syst. 5(11), 2100095 (2021). Crossref
3. Y. Ma, Q. Hao, B. Poudel, Yu. Lan, B. Yu, D. Wang, G. Chen, Zh. Ren. Nano Lett. 8 (8), 2580 (2008). Crossref
4. CRC Handbook of Thermoelectrics (Ed. by D. M. Rowe). CRC Press, Boca Raton, FL (1995).

5. H. J. Goldsmid. Thermoelectric Refrigeration. Plenum Press, New York (1964). Crossref
6. Semiconductors and Semimetals (Ed. by T. M. Tritt). Academic Press, San Diego, CA (2001).
7. D. Beretta, N. Neophytou, J. M. Hodges, M. G. Kanatzidis, D. Narducci, M. Martin-Gonzalez, M. Beekman, B. Balke, G. Cerretti, W. Tremel, A. Zevalkink, A. I. Hofmann, C. Müller, B. Dörling, M. Campoy-Quiles, M. Caironi. Mater. Sci. Eng. R. 138, 100501 (2019). Crossref
8. G. Guelou et al. J. Mater. Chem. C. 9, 773 (2021). Crossref
9. W.-D. Liu, L. Yang, Z.-.G. Chen, J. Zou. Adv. Mater. 32, 1905703 (2020). Crossref
10. T. Wang, T. Guo, H. Wang, C. Wang, Sci. China Mater. 63, 8 (2020). Crossref
11. C. Ou, A. L. Sangle, A. Datta, Q. Jing, T. Busolo, T. Chalkley, V. Narayan, S. Kar-Narayan. ACS Appl. Mater. Interfaces. 10, 19580 (2018). Crossref
12. K. Kanahashi, J. Pu, T. Takenobu. Adv. Energy Meter. 10, 1902842 (2020). Crossref
13. N. Jaziri, et al. Energy Rep. 6, 264 (2020). Crossref
14. J. Yan, X. Liao, D. Yan, Y. Chen. J. Microelectromech. Syst. 27, 1 (2018). Crossref
15. P. Qiu, Y. Zhu, Y. Qin, X. Shi, L. Chen. APL Mater. 4 (10), 104805 (2016). Crossref
16. M. M. Kubenova, K. A. Kuterbekov, M. Kh. Balapanov, R. Kh. Ishembetov, A. M. Kabyshev, K. Zh. Bekmyrza. Nanomaterials. 11, 2238 (2021). Crossref
17. X. Li, C. Hu, X. Kang, Q. Len, Y. Xi, K. Zhang, H. J. Mater. Chem. A. 1, 13721 (2013). Crossref
18. M. H. Balapanov, R. H. Ishembetov, B. M. Ahmetgaliev, K. A. Kuterbekov, R. SH. Palymbetov, S. M. Sahabaeva, R. A. Yakshibaev. Vestnik Bashkirskogo universiteta. 25, 794 (2020). Crossref
19. M. Kh. Balapanov, R. Kh. Ishembetov, K. A. Kuterbekov, A. Kh. Baisheva, R. Sh. Palymbetov, S. M. Sakhabaeva, M. M. Kubenova, R. A. Yakshibaev. Letters on materials. 10 (4), 439 (2020). (in Russian) Crossref
20. E. H. Roseboom. Econ. Geol. 61, 641 (1966). Crossref
21. S.-C. Ur, I.-H. Kim, P. Nash. J. Mater. Sci. 42, 2143 (2007). Crossref
22. M. H. Balapanov, R. H. Ishembetov, B. M. Ahmetgaliev, K. A. Kuterbekov, R. Sh. Palymbetov, S. M. Sahabaeva, R. A. YAkshibaev, M. M. Kubenova. Sbornik trudov V Mezhdunar. nauch.-prakt. konf. Respublika Bashkortostan, Sterlitamak (2021) pp 34 – 40.
23. D. J. Chakrabarti, D. E. Laughlin. Phase Equilibria. 4 (3), 254 (1983). Crossref
24. J. B. Rivest, L.-K. Fong, P. K. Jain, M. F. Toney, A. P. Alivisatos. J. Phys. Chem. Lett. 2, 2402 (2011). Crossref
25. J. Gong, P. K. Jain. Nature commun. 10, 3285 (2019). Crossref
26. S. M. Sakhabayeva, M. Kh. Balapanov, K. A. Kuterbekov, R. Kh. Ishembetov, M. M. Kubenova, Sh. G. Giniyatova, S. A. Nurkenov, B. M. Akhmetgaliev, M. Kh. Zeleev, R. A. Yakshibaev, G. S. Seisenbayeva. Eurasian Journal of Physics and Functional Materials. 6 (1), 71 (2022). Crossref
27. S. M. Kauzlarich, Sh. R. Brown, G. J. Snyder. Dalton Trans. 21, 2099 (2007). Crossref
28. P. Qiu, X. Shi, L. Chen. Energy Storage Materials. 85 (3), 85 (2016). Crossref
29. H. L. Liu, X. Shi, F. F. Xu, L. L. Zhang, W. Q. Zhang, L. D. Chen, Q. Li, C. Uher, T. Day, G. J. Snyder. Nat. Mater. 11 (5), 422 (2012). Crossref
30. S. M. Sakhabayeva, M. Kh. Balapanov, K. A. Kuterbekov, Sh. G. Giniyatova, M. M. Kubenova, R. Sh. Palymbetov, R. H. Ishembetov, Y. H. Yulaeva. Recent Contibutions to Physics. 79 (4), 72 (2021). Crossref